Eur. Phys. J. A **25**, 293–298 (2005)
DOI 10.1140/epja/i2005-10095-1

THE EUROPEAN PHYSICAL JOURNAL A

Neutron stars with isovector scalar correlations

B. Liu[1,2], H. Guo[1,3], M. Di Toro[4,a], and V. Greco[4,5]

[1] Center of Theoretical Nuclear Physics, National Laboratory of Heavy Ion Accelerator, Lanzhou 730000, PRC
[2] Institute of High Energy Physics, Chinese Academy of Sciences, Beijing 100039, PRC
[3] Department of Technical Physics, Peking University, Beijing 100871, PRC
[4] Laboratori Nazionali del Sud, Via S. Sofia 44, I-95123 Catania, and University of Catania, Italy
[5] Cyclotron Institute, Texas A&M University, College Station, TX, USA

Received: 13 January 2005 /
Published online: 25 August 2005 –
Communicated by A. Molinari

Abstract. Neutron stars with the isovector scalar δ-field are studied in the framework of the relativistic mean-field (RMF) approach in a pure-nucleon–plus–lepton scheme. The δ-field leads to a larger repulsion in dense neutron-rich matter and to a definite splitting of proton and neutron effective masses. Both features are influencing the stability conditions of the neutron stars. Two parametrizations for the effective nonlinear Lagrangian density are used to calculate the nuclear equation of state (EOS) and the neutron star properties, and compared to correlated Dirac-Brueckner results. We conclude that in order to reproduce reasonable nuclear structure and neutron star properties within a RMF approach, a density dependence of the coupling constants is required.

PACS. 21.65.+f Nuclear matter – 21.30.Fe Forces in hadronic systems and effective interactions – 26.60.+c Nuclear matter aspects of neutron stars – 97.60.Jd Neutron stars

A relativistic mean-field (RMF) approach to nuclear matter with the coupling to an isovector scalar field, a virtual $a_0(980)$ δ-meson, has been employed to study various topics related with low-density asymmetric nuclear matter, including its linear response [1–3], and with heavy-ion collisions at intermediate energies, where larger density and momentum regions can be probed [4–6]. In this work the analysis of the contribution of a δ-field is extended to study the impact on neutron star properties. We also aim at a discussion about the effective interaction that is more appropriate for the description of dense matter, including the symmetric part. To this end we will make a comparison between two parametrizations for the isoscalar part of the interaction and for each of them we will discuss the cases with and without the inclusion of an isovector scalar field.

A Lagrangian density of the interacting many-particle system consisting of nucleons, isoscalar (scalar σ, vector ω), and isovector (scalar δ, vector ρ) mesons is the starting point of the RMF theory,

$$\begin{aligned}\mathcal{L} = \bar{\psi}\Big[i\gamma_\mu\partial^\mu - (M - g_\sigma\phi - g_\delta\vec{\tau}\cdot\vec{\delta}) - g_\omega\gamma_\mu\omega^\mu \\ -g_\rho\gamma^\mu\vec{\tau}\cdot\vec{b}_\mu\Big]\psi + \frac{1}{2}(\partial_\mu\phi\partial^\mu\phi - m_\sigma^2\phi^2) - U(\phi) \\ +\frac{1}{2}m_\omega^2\omega_\mu\omega^\mu + \frac{1}{2}m_\rho^2\vec{b}_\mu\cdot\vec{b}^\mu + \frac{1}{2}(\partial_\mu\vec{\delta}\cdot\partial^\mu\vec{\delta} - m_\delta^2\vec{\delta}^2) \\ -\frac{1}{4}F_{\mu\nu}F^{\mu\nu} - \frac{1}{4}\vec{G}_{\mu\nu}\vec{G}^{\mu\nu}, \qquad (1)\end{aligned}$$

where ϕ is the ϕ-meson field, ω_μ is the ω-meson field, $\vec{b}_\mu$ is ρ-meson field, $\vec{\delta}$ is the isovector scalar field of the δ-meson. $F_{\mu\nu} \equiv \partial_\mu\omega_\nu - \partial_\nu\omega_\mu$, $\vec{G}_{\mu\nu} \equiv \partial_\mu\vec{b}_\nu - \partial_\nu\vec{b}_\mu$, and the $U(\phi)$ is a nonlinear potential of the σ-meson: $U(\phi) = \frac{1}{3}a\phi^3 + \frac{1}{4}b\phi^4$.

The field equations in a mean-field approximation (MFA) are

$$\begin{aligned}(i\gamma_\mu\partial^\mu - (M - g_\sigma\phi - g_\delta\tau_3\delta_3) \\ -g_\omega\gamma^0\omega_0 - g_\rho\gamma^0\tau_3 b_0)\psi = 0, \\ m_\sigma^2\phi + a\phi^2 + b\phi^3 = g_\sigma\langle\bar{\psi}\psi\rangle = g_\sigma\rho_s, \\ m_\omega^2\omega_0 = g_\omega\langle\bar{\psi}\gamma^0\psi\rangle = g_\omega\rho, \\ m_\rho^2 b_0 = g_\rho\langle\bar{\psi}\gamma^0\tau_3\psi\rangle = g_\rho\rho_3, \\ m_\delta^2\delta_3 = g_\delta\langle\bar{\psi}\tau_3\psi\rangle = g_\delta\rho_{s3}, \qquad (2)\end{aligned}$$

where $\rho_3 = \rho_p - \rho_n$ and $\rho_{s3} = \rho_{sp} - \rho_{sn}$, ρ and ρ_s are the baryon and the scalar densities, respectively.

Neglecting the derivatives of mesons fields, the energy-momentum tensor in the MFA is given by

$$\begin{aligned}T_{\mu\nu} = i\bar{\psi}\gamma_\mu\partial_\nu\psi + \Big[\frac{1}{2}m_\sigma^2\phi^2 + U(\phi) + \frac{1}{2}m_\delta^2\vec{\delta}^2 \\ -\frac{1}{2}m_\omega^2\omega_\lambda\omega^\lambda - \frac{1}{2}m_\rho^2\vec{b_\lambda}\vec{b^\lambda}\Big]g_{\mu\nu}. \qquad (3)\end{aligned}$$

The equation of state (EOS) for nuclear matter at $T = 0$ is given by the diagonal components of the energy-momentum tensor. The energy density is given by

[a] e-mail: ditoro@lns.infn.it

the T_{00} component:

$$\epsilon = \langle T^{00} \rangle = \sum_{i=n,p} 2 \int \frac{\mathrm{d}^3k}{(2\pi)^3} E_i^\star(k) + \frac{1}{2} m_\sigma^2 \phi^2 + U(\phi) + \frac{1}{2} m_\omega^2 \omega_0^2 + \frac{1}{2} m_\rho^2 b_0^2, + \frac{1}{2} m_\delta^2 \delta_3^2, \quad (4)$$

and the pressure by the other diagonal components:

$$p = \frac{1}{3} \sum_{i=1} \langle T^{ii} \rangle = \sum_{i=n,p} \frac{2}{3} \int \frac{\mathrm{d}^3k}{(2\pi)^3} \frac{k^2}{E_i^\star(k)} - \frac{1}{2} m_\sigma^2 \phi^2 - U(\phi) + \frac{1}{2} m_\omega^2 \omega_0^2 + \frac{1}{2} m_\rho^2 b_0^2 - \frac{1}{2} m_\delta^2 \delta_3^2, \quad (5)$$

where $E_i^\star = \sqrt{k^2 + {M_i^\star}^2}$, $i = p, n$. The nucleon effective masses are, respectively,

$$M_p{}^\star = M - g_\sigma \phi - g_\delta \delta_3, \quad (6)$$

and

$$M_n{}^\star = M - g_\sigma \phi + g_\delta \delta_3. \quad (7)$$

The nucleon chemical potentials μ_i are given in terms of the vector meson mean fields,

$$\mu_i = \sqrt{k_{\mathrm{F}_i}^2 + {M_i^\star}^2} + g_\omega \omega_0 \mp g_\rho b_0 \quad (+ \text{ proton}, - \text{ neutron}), \quad (8)$$

where the Fermi momentum k_{F_i} of the nucleon is related to its density, $k_{\mathrm{F}_i} = (3\pi^2 \rho_i)^{1/3}$.

Since we are interested to the effects of the nuclear equation of state, we will consider only pure nucleonic (+ lepton) neutron star structures, *i.e.* without strangeness bearing baryons and even deconfined quarks, see the recent nice review [7] and ref. [8]. In particular we will use two models for the neutron star composition: pure neutron and β-stable matter. In the latter case we limit the constituents to be neutrons, protons and electrons. Then the composition is determined by the request of charge neutrality and β-equilibrium. The (npe^-) matter is indeed the most important β-stable nucleon + lepton matter at low temperature.

The chemical-potential equilibrium condition for the (npe^-) system can be written as

$$\mu_e = \mu_n - \mu_p \ . \quad (9)$$

The charge neutrality condition is

$$\rho_e = \rho_p = X_p \rho \ , \quad (10)$$

where $X_p = Z/A = \rho_p/\rho$ is the proton fraction (asymmetry parameter $\alpha = 1 - 2X_p$), and ρ is the total baryon density. The electron density ρ_e in the ultrarelativistic limit for noninteracting electrons can be denoted as a function of its chemical potential

$$\rho_e = \frac{1}{3\pi^2} \mu_e^3 \ , \quad (11)$$

Table 1. Parameter sets.

Parameter	Set A		Set B	
	NLρ	NL$\rho\delta$	NLρ	NL$\rho\delta$
f_σ (fm^2)	10.32924	10.32924	15.61225	15.61225
f_ω (fm^2)	5.42341	5.42341	10.40068	10.40068
f_ρ (fm^2)	0.94999	3.1500	1.09659	3.08509
f_δ (fm^2)	0.00	2.500	0.00	2.400
A (fm^{-1})	0.03302	0.03302	0.00999	0.00999
B	−0.00483	−0.00483	−0.002669	−0.002669

Table 2. Saturation properties of nuclear matter.

Parameter sets	A	B
ρ_0 (fm^{-3})	0.16	0.148
E/A (MeV)	−16.0	−16.299
K (MeV)	240.0	271.7
E_{sym} (MeV)	31.3	33.7
M^*/M	0.75	0.60

where $\mu_e = \sqrt{k_{\mathrm{F}_e}^2 + m_e^2}$. The X_p can be obtained by using eqs. (8)-(11). The X_p is related to the nuclear symmetry energy E_{sym}

$$3\pi^2 \rho X_p - [4E_{\mathrm{sym}}(\rho)(1 - 2X_p)]^3 = 0. \quad (12)$$

In the presence of a coupling to an isovector scalar δ-meson field, the expression for the symmetry energy has a simple transparent form, see [2,3]:

$$E_{\mathrm{sym}}(\rho) = \frac{1}{6} \frac{k_{\mathrm{F}}^2}{E_{\mathrm{F}}} + \frac{1}{2} \left[f_\rho - f_\delta \left(\frac{M^\star}{E_{\mathrm{F}}^\star} \right)^2 \right] \rho \ , \quad (13)$$

where $M^\star = M - g_\sigma \phi$ and $E_{\mathrm{F}}{}^\star = \sqrt{k_{\mathrm{F}}^2 + {M^\star}^2}$, and $f_i \equiv g_i^2/m_i^2$ with $i = \rho, \delta$. The E_{sym} and the EOS for the β-stable (npe^-) matter at $T = 0$ can be estimated by using the obtained values of X_p. Equilibrium properties of the neutron stars can be finally studied by solving Tolmann-Oppenheimer-Volkov (TOV) equations [9,10] with the derived nuclear EOS as an input [7].

We will consider two cases for the isovector part of the interaction: a case with only a ρ-field (NLρ) and another with both ρ and δ-fields (NL$\rho\delta$). In the NLρ case the symmetry energy at saturation density fixes the f_ρ coupling. In the NL$\rho\delta$ the f_δ coupling is fixed from Dirac-Brueckner estimations, *i.e.* $f_\delta \simeq 2.5$ fm^2, and the f_ρ coupling by symmetry energy value at saturation density, see the detailed discussions in refs. [2,3].

In order to make a comparison, two parameter sets for the isoscalar part are used. The coupling constants, $f_i \equiv g_i^2/m_i^2$, $i = \sigma, \omega, \rho, \delta$, and the two parameters of the σ self-interacting terms, $A \equiv a/g_\sigma^3$ and $B \equiv b/g_\sigma^4$, are reported in table 1. The corresponding properties of nuclear matter are listed in table 2. The first, Set A, is more suitable at high densities where it appears closer to various

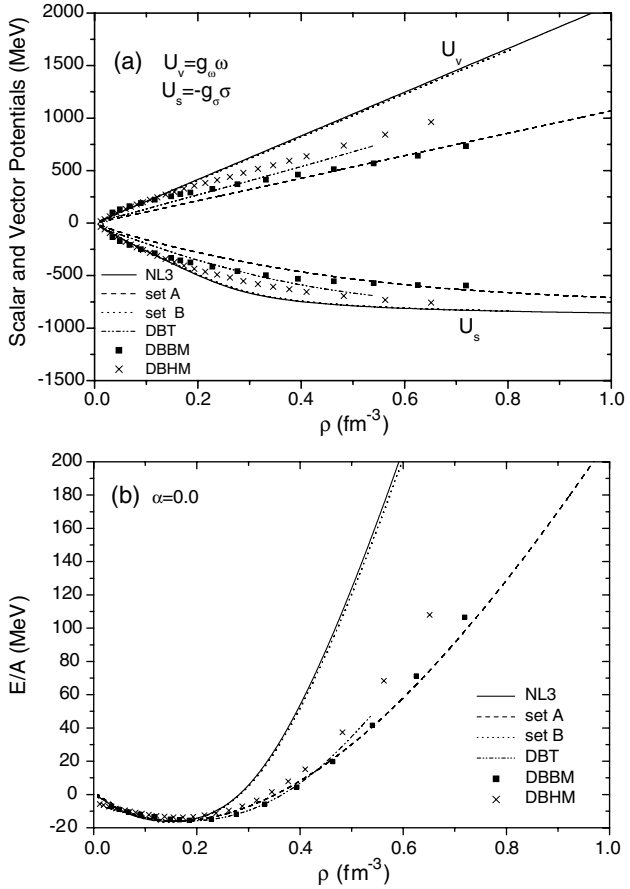

Fig. 1. (a) Scalar and vector potentials *vs.* the baryon density; (b) binding energy as a function of the baryon density for symmetric nuclear matter. See text.

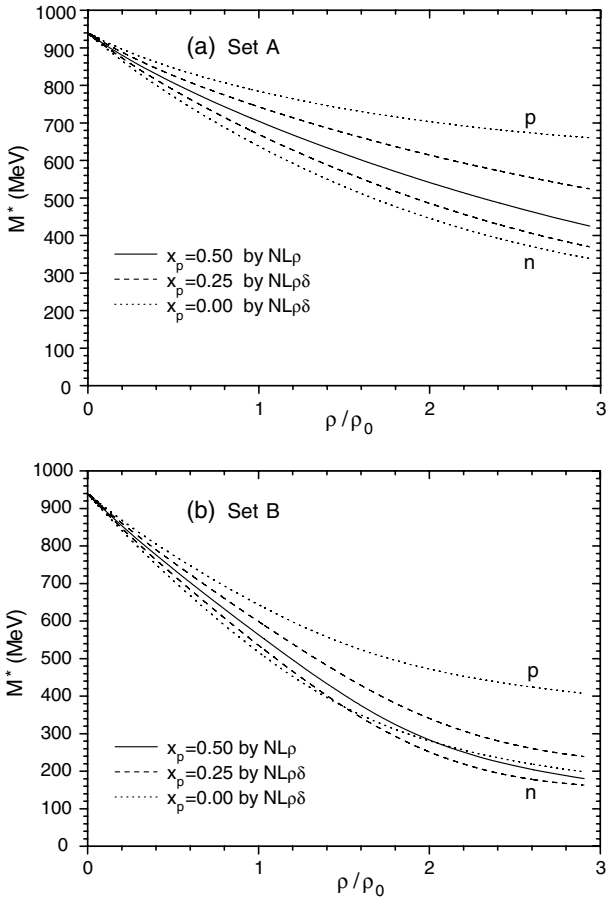

Fig. 2. Neutron and proton effective masses *vs.* the baryon density for some values of the proton fraction: (a) for Set A and (b) for Set B. See text.

Dirac-Brueckner predictions. In fact, recently this interaction has been used with success to describe reaction observables in RMF transport simulations of relativistic heavy-ion collisions, where high densities and momenta are reached [4–6]. The second, Set B, for the isospin-zero case is taken from the NL3 parametrization [11], obtained by fitting properties of symmetric nuclear matter at saturation density and of finite nuclei. Then the NLρ case is exactly like NL3, where the isovector scalar channel is not included. The NL$\rho\delta$ is obtained, similarly to Set A, fixing $f_\delta = 2.4$ fm^2 and requiring $E_{\rm sym}(\rho_0) = 33.7$ MeV. Notice that $E_{\rm sym}(\rho_0) = 37.4$ MeV in NL3; however this does not affect the message of the present work.

In ref. [5] it has been shown that the good description of finite nuclei, even exotic, is kept also when the isovector scalar channel is included, normally not present in the NL3 Lagrangian.

We first use the two parametrizations to calculate the scalar and the vector potentials, and the binding energy E/A for symmetric nuclear matter ($\alpha = 0.0$) as a function of baryon density. The results are presented in fig. 1 together with the results from various Dirac-Brueckner-Hartree-Fock calculations.

The relativistic DBHF approach is a microscopic model describing a many-body system with correlations, that has been extensively used to study the nuclear-matter properties [12–17]. In order to make a comparison with the RMFT, in fig. 1 we also report different results within the DBHF approaches, the relativistic Dirac-Brueckner calculations by Brockmann and Machleidt [12], denoted as DBBM, the Dirac-Brueckner T-matrix calculations [13], denoted as DBT, and the Dirac-Brueckner results by ter Haar and Malfliet [14], denoted as DBHM.

From fig. 1(a) we see that the scalar and vector potentials for the isoscalar channels, given by Set B (*i.e.* the NL3 $\sigma\omega$ couplings) in low-density regions are consistent with the correlated Dirac-Brueckner results, while the results given by Set A are in better agreement in high-density regions.

The dotted line in fig. 1(b) denotes the EOS of symmetric nuclear matter given by Set B, in full overlap with the solid line given by the NL3 interaction. It shows a nice agreement with correlated relativistic predictions at low densities but is clearly too repulsive with increasing density. At variance fig. 1(b) also shows that, as expected, the EOS of symmetric nuclear matter given by Set A is more consistent with that given by Dirac-Brueckner calculations, in particular for the DBT and DBBM estimations, in high-density regions up to about three-four times

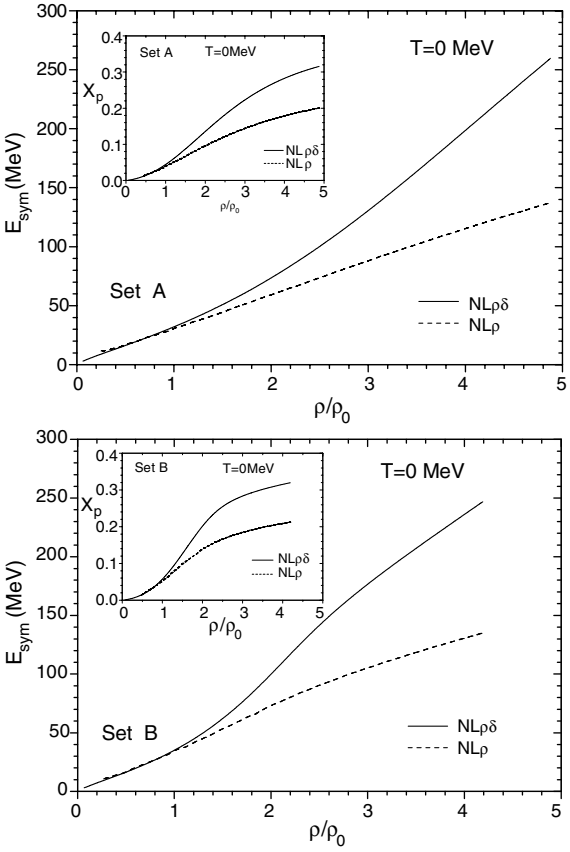

Fig. 3. Symmetry energy *vs.* the baryon density at $T = 0$ MeV for Set A (upper panel) and for Set B (lower panel). In the insert is the corresponding proton fraction, see text.

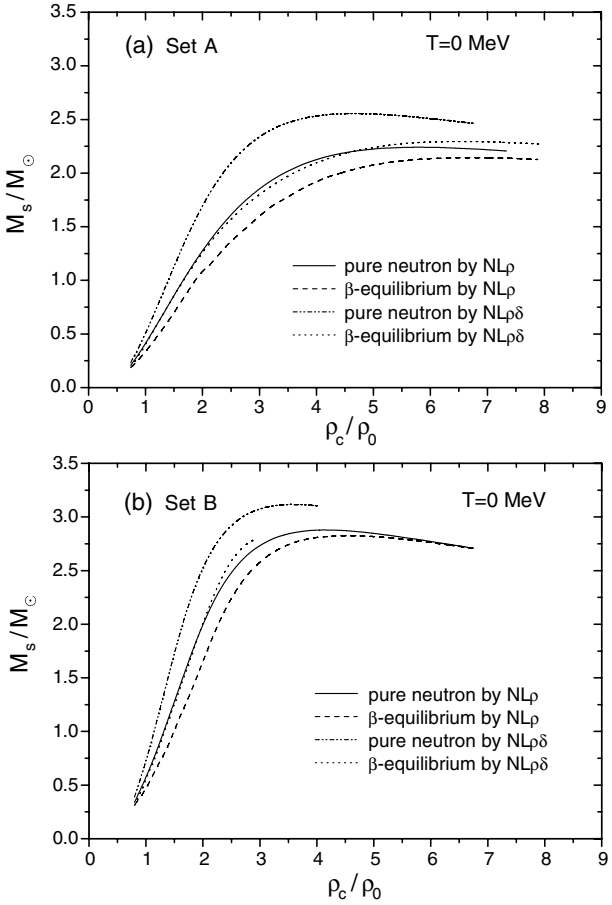

Fig. 4. Mass of the neutron star as a function of the central density of the neutron star by Set A and Set B, respectively.

normal density. Such a different behavior at high baryon density, in connection to the large difference in nucleon effective masses, will strongly influence the neutron star structure.

Relativistic heavy-ion collisions can provide crucial information about the EOS of nuclear matter. The investigation of nuclear EOS at high densities is one of the driving forces for studying heavy-ion reactions. The authors of ref. [15] use different DBHF approaches to study the collective flow of heavy-ion collisions. It is shown that the softer DBT choice is in better agreement with experimental data of relativistic collisions, at least up to a few A GeV beam energies, where densities up to $2.5\rho_0$ can be reached in the interacting zone. In general very accurate analysis of relativistic-collisions data favor the predictions of a softer EOS at high densities [18,19]. We remark from fig. 1(b) that for symmetric matter the DBT is quite close to our Set-A parametrization, at least up to about $3\rho_0$.

For the isovector channels one can see from eqs. (6) and (7) that the presence of the δ-field leads to proton and neutron effective mass splitting. In fig. 2 we present the baryon density dependence of n, p effective masses for different proton fractions for the two parameter sets. The solid lines in fig. 2 are the nucleon effective mass for symmetric nuclear matter ($X_p = 0.5$).

Figure 2(a) shows that the proton and the neutron effective masses given by Set A decrease slowly with increasing baryon density, at variance with Set B that presents a much faster decrease, fig. 2(b). This main difference between the two A and B parametrizations, is actually coming from the isoscalar part. When coupled to the splitting due to the isovector δ-field it will have large effects on the n star equilibrium features.

The density dependence of symmetry energy for the two parameter sets is reported in fig. 3. For both cases we see a similar behavior of $E_{\rm sym}$ at sub-saturation densities for NLρ and NL$\rho\delta$ models. With increasing baryon density ρ, however, the differences arising from the presence of the δ-meson in the isovector channel become more pronounced for both A and B parametrizations. This is due to the quenching factor $(M^\star/E^\star_{\rm F})^2$ for the attractive δ contribution in eq. (13) in high-density regions, see refs. [2,3].

We note that in spite of the same isovector coupling constants, at high density Set B gives a larger symmetry energy. This is related to the larger contribution of the kinetic term in the r.h.s. of eq. (13) due to the faster decrease of the effective nucleon mass. This represents a nice example of how the isovector part of the nuclear EOS can be influenced by the isoscalar channels due to the Fermi correlations.

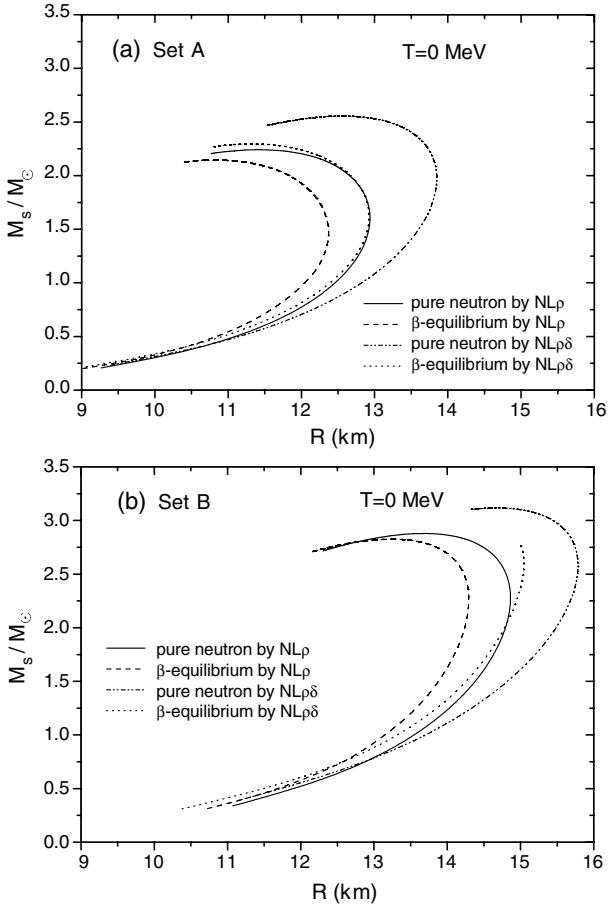

Fig. 5. Mass of the neutron star as a function of the radius of the neutron star for Set A (upper pannel) and Set B (lower panel), respectively.

In the inserts of fig. 3 we show the corresponding proton fractions X_p at β-equilibrium, eq. (12). Due to the stiffer nature of the symmetry energy in the NL$\rho\delta$ cases, in both parametrizations we see a decrease of the $\rho_{\rm Urca}$, *i.e.* of the baryon density corresponding to the value $X_p = 1/9$ that makes possible a direct Urca process, see [7].

At this point we can calculate the predictions for equilibrium properties of neutron stars just solving the TOV equations [9,10]. The main results are presented in figs. 4 and 5.

Figure 4 displays the neutron star mass as a function of the central density of the star given by the two parameter sets, for the two compositions, pure neutron and the β-equilibrium (npe^-) matter.

Figures 4(a) and (b) both show that the maximum masses of the β-equilibrium star are smaller than in the pure-neutron case due to the presence of a proton fraction and therefore of a smaller symmetry repulsion. Consistently, the corresponding central densities are larger. A related effect is that the mass of the (npe^-) star, given by the NL$\rho\delta$ model, decreases more quickly with increasing density than that given by the NLρ choice, *i.e.* we have a lower-density instability onset. This is just because the introduction of the δ coupling increases the equilibrium proton fraction at high baryon densities, see the inserts in fig. 3.

Table 3. Maximum mass, corresponding radius and central density of the star given by the two parameter sets.

Neutron star	Properties	Set A		Set B	
		NLρ	NL$\rho\delta$	NLρ	NL$\rho\delta$
Pure neutron	$(Ms/M\odot)_{\rm max}$	2.24	2.56	2.88	3.12
	ρ_c/ρ_0	5.75	4.65	4.12	3.55
	R (km)	11.44	12.56	13.70	14.69
(npe^-) matter	$(Ms/M\odot)_{\rm max}$	2.14	2.30	2.83	
	ρ_c/ρ_0	6.77	6.49	4.54	
	R (km)	10.80	11.33	13.25	

The larger stiffness of the symmetry energy in the NL$\rho\delta$ cases, in both parametrizations, can be directly seen in the fact that the corresponding curves are always above the ones without the δ coupling. This implies larger maximum masses and smaller central densities. As a consequence, we systematically see that the results for the (npe^-) composition in the NL$\rho\delta$ models are approximately equivalent to the ones for the pure-neutron matter in NLρ choices.

Figure 4(b) presents a qualitatively new feature of Set-B results: the lack of solution (maximum mass) in the β-equilibrium case for the NL$\rho\delta$ model. The fast decrease of the neutron effective mass, see fig. 2(b), prevents the chemical-potential equilibrium condition for the (npe^-) matter from being satisfied at densities around $3\rho_0$.

Figure 5 reports the correlation between neutron star mass and radius given by the two parameter sets, respectively, for the two cases, pure neutron and (npe^-) matter. Figure 5 shows that the contribution of the δ-field to the neutron stars in high-density regions is quite remarkable. In particular, we note that we systematically have larger masses and radii and lower central densities, as expected from the larger symmetry pressure.

All the estimated maximum masses and the corresponding central densities and radii of the neutron stars are reported in table 3.

We note that the difference between the two, A and B, parametrizations, in the neutron star predictions, is largely due to the isoscalar structure of the interactions, see fig. 1. The B parametrization is much stiffer in high-density regions and this leads to differences in the neutron star masses, radii and central densities. The comparison between the results given by the two sets shows that Set B (*i.e.* the NL3 forces) can be good at low densities below saturation density and it has serious problems at high densities, while Set A is a good choice for the EOS of nuclear matter in larger-density regions, which is consistent with what pointed out by refs. [19,20]. In a sense, all of that just shows that density-dependent RMF parametrizations are necessary and they should reproduce the B-type at low densities and A-type at high densities. This has been already emphasized in the work of ref. [21]. While results of Density-Dependent (DD)

parametrizations and of the NL3 forces agree very well below the saturation density, the EOS of DD interactions at supra-normal densities shows a much softer behavior, similar to DBHF calculations and in better agreement with heavy-ion collision (HIC) data, see also ref. [5].

In any case our calculations show that the δ-field provides significant contributions to the neutron star structure for the stiffness of the symmetry energy and the neutron/proton mass splitting in high-density regions. The proton fraction in the β-equilibrium matter is much larger than that in the no δ-field case. Moreover, we can see from fig. 4(b) and fig. 5(b) that we do not have solutions in the (npe^-) case for Set B with NL$\rho\delta$ isovector interaction. This represents a quite dramatic effect of the splitting of neutron/proton effective masses at high densities, on top of the larger nucleon mass decrease of the B parametrizations, see fig. 2. The neutron chemical potential is then not able to satisfy the β-equilibrium conditions of the (npe^-) matter. The contribution of the δ-field for strongly isospin-asymmetric dense matter is important and it cannot be neglected.

With reference to neutron star properties we study the EOS for dense asymmetric matter in the RMF frame with two different parameter sets for the Lagrangian density. Set B is close to the NL3 parametrization which has been proposed to describe finite nuclei properties. Since the proton and especially the neutron effective masses decrease quickly with increasing baryon density, Set B cannot provide the EOS needed in high-density regions for the (npe^-) star. This means that in general the B parametrization seems to have serious problems at high densities, as already remarked from HIC studies [19]. Though the B parametrization can be good for the EOS at low densities, below and around saturation, it is too stiff in high-density regions, in particular there is no solution for the (npe^-) case with the δ-field. So Set B is not suitable for the case of dense matter. We require a softer EOS at high densities, and indeed the softer Dirac-Brueckner predictions, in particular the DBT one, are in better agreement with relativistic-collisions data. Our A parametrization, including the isovector scalar δ-field, is quite close to the DBT and it has been shown to lead to good predictions in transport simulations for heavy-ion collisions at intermediate energies [4–6]. It appears then quite appropriate for the nucleonic part of the approach to neutron star properties. In this respect we note that quite extended neutron star structure calculations have been recently performed just using our Set-A Lagrangian [22].

This project is supported by the National Natural Science Foundation of China under Grant No. 10275002, the INFN of Italy, and the Major State Basic Research Developing Program with Grant No. G2000077400.

References

1. S. Kubis, M. Kutschera, Phys. Lett. B **399**, 191 (1997).
2. B. Liu, V. Greco, V. Baran, M. Colonna, M. Di Toro, Phys. Rev. C **65**, 045201 (2002).
3. V. Greco, M. Colonna, M. Di Toro, F. Matera, Phys. Rev. C **67**, 015203 (2003).
4. V. Greco *et al.*, Phys. Lett. B **562**, 215 (2003).
5. T. Gaitanos *et al.*, Nucl. Phys. A **732**, 24 (2004).
6. T. Gaitanos, M. Colonna, M. Di Toro, H.H. Wolter, Phys. Lett. B **595** , 209 (2004).
7. J.M. Lattimer, M. Prakash, Science **304**, 536 (2004).
8. C. Maieron, M. Baldo, G.F. Burgio, H.J. Schultze, Phys. Rev. D **70**, 043010 (2004).
9. R.C. Tolman, Phys. Rev. **55**, 364 (1939)
10. J.R. Oppenheimer, G.M. Volkoff, Phys. Rev. **55**, 374 (1939).
11. G.A. Lalazissis, J. König, P. Ring, Phys. Rev. C **55**, 540 (1997).
12. R. Brockmann, R. Machleidt, Phys. Rev. C **42**, 1965 (1990).
13. T. Gross-Boelting, C. Fuchs, A. Faessler, Nucl. Phys. A **648**, 105 (1999).
14. B. ter Haar, R. Malfliet, Phys. Rep. **149**, 207 (1987).
15. T. Gaitanos, C. Fuchs, H.H. Wolter, A. Faessler, Eur. Phys. J. A **12**, 421 (2001).
16. A.B. Santra, U. Lombardo, Phys. Rev. C **62**, 018202 (2001).
17. F. de Jong, H. Lenske, Phys. Rev. C **57**, 3099 (1998).
18. P. Danielewicz, Nucl. Phys. A **673**, 375 (2000).
19. P. Danielewicz, R. Lacey, W.G. Lynch, Science **298**, 1592 (2002).
20. A.M.S. Santos, D.P. Menezes, Phys. Rev. C **69**, 045803 (2004).
21. S. Typel, H.H. Wolter, Nucl. Phys. A **656**, 331 (1999).
22. D.P. Menezes, C. Providencia, Phys. Rev. C **70**, 058801 (2004).